ARTICLE

Check for updates

Towards phase-stabilized Fourier domain mode-locked frequency combs

Christin Grill [1], Torben Blömker[1], Mark Schmidt [2], Dominic Kastner[1], Tom Pfeiffer[1,3], Jan Philip Kolb[1], Wolfgang Draxinger [1], Sebastian Karpf[1], Christian Jirauschek [2] & Robert Huber [1✉]

Fourier domain mode-locked (FDML) lasers are some of the fastest wavelength-swept light sources, and used in many applications like optical coherence tomography (OCT), OCT endoscopy, Raman microscopy, light detection and ranging, and two-photon microscopy. For a deeper understanding of the underlying laser physics, it is crucial to investigate the light field evolution of the FDML laser and to clarify whether the FDML laser provides a frequency comb structure. In this case, the FDML would output a coherent sweep in frequency with a stable phase relation between output colours. To get access to the phase of the light field, a beat signal measurement with a stable, monochromatic laser is performed. Here we show experimental evidence of a well-defined phase evolution and a comb-like structure of the FDML laser. This is in agreement with numerical simulations. This insight will enable new applications in jitter-free spectral-scanning, coherent, synthetic THz-generation and as metrological time-frequency ruler.

[1] Institute of Biomedical Optics, University of Lübeck, 23562 Lübeck, Germany. [2] Department of Electrical and Computer Engineering, Technical University of Munich, 80333 Munich, Germany. [3] Optores GmbH, Gollierstr. 70, 80339 Munich, Germany. ✉email: robert.huber@uni-luebeck.de

Fourier domain mode-locking (FDML) is a laser operating regime, which was originally developed for optical coherence tomography (OCT) in 2005[1,2]. OCT is an optical imaging modality with many clinical applications[3]. We demonstrated the advantages of FDML lasers in fields such as ophthalmology[4–7], cardiovascular imaging[8–10], dermatology[11] and neurosurgery[12]. The speciality of the FDML laser is a coherent wavelength-swept laser output[13,14] which conceptually can be understood as a highly chirped broadband light field: In analogy to a femtosecond mode-locked laser, which is characterized by a pulse repetition rate and a short impulse, generated by phase-stable summation of many mode-locked laser modes, the FDML laser operates in a different yet analogous regime. It also provides a repetitive behaviour, given by the wavelength sweep rate. However, in contrast to the modes each having a distinct, yet locked phase, the light field of the FDML laser is characterized by a swept phase: The phase is chirped to generate a swept wavelength light field where the colour is continuously changed over time (temporal rainbow). As these colours bear a phase relation between each other, the name Fourier domain mode-locking was chosen in contrast to conventional amplitude mode-locking.

The broadband nature and the temporal access to the individual colours have enabled spectroscopic techniques like absorption spectroscopy[15], stimulated Raman spectroscopy[16] and hyperspectral Raman microscopy[17]. Recently, the excellent sweep characteristic was also employed for fibre Bragg grating sensing[18], and inertia free beam scanning employing spectro-temporal encoding in two-photon microscopy[19,20] and light detection and ranging[21]. The novel operating regime was also the subject of many theoretical works investigating the phase evolution, coherence properties, nonlinear behaviour, or polarization dynamics[13,22–26].

Here, we investigate experimentally whether the FDML laser constitutes a frequency comb[27]. Therefore, we generated beat signals between a monochromatic laser with a narrow linewidth and the FDML laser. Comparison with numerical simulations confirms the comb-structure and that the comb spacing is given by the FDML sweep rate. In conclusion, even FDML frequency combs with a stabilized carrier-envelope phase can be possible in the future.

Results and discussion
Experimental setup, performance and analysis concept. The experimental setup is depicted in Fig. 1. To test the FDML frequency comb hypothesis, we interrogated the optical phase by beating the optical light field of the FDML laser (Fig. 1a) against a frequency normal, i.e. the 1st continuous wave (CW) laser in Fig. 1b. We measured the beat signal between a home-built, narrowband CW laser as our frequency normal and an FDML laser around 1300 nm in a highly coherent, sweet-spot operation[28,29]. To guarantee optimal operation of the monochromatic reference laser, we simultaneously recorded the beat note signal of this laser with a second, identical laser (Fig. 1c). For monitoring and setup, the time-averaged spectrum of the FDML laser in this case sweeping over 80 nm (Fig. 1d) is measured. Figure 1e shows the oscilloscope trace of photodiode 1 for a duration of six sweeps. We see the 1 μs long signals from the FDML sweeps at a level of approximately 0.15 V and the needle-like signatures, where a beat signal is measurable. The calculated radio frequency spectrum from the beat signal between the two CW lasers (Fig. 1f) characterized the optical performance of the CW lasers during the short measurement time and gave access to an upper limit of their linewidth and therefore of their spectral stability and the appearance of mode hops. We only utilized those beat note signals where the frequency reference was of sufficiently narrowband character (less than 30 kHz). Additionally, the optical spectrum of both overlaid CW lasers is measured to adjust the wavelengths close to each other (Fig. 1g).

The filter of the FDML laser is driven sinusoidally (Fig. 2a), since a filter rapidly driven in resonance is preferred for FDML applications, where a high repetition rate is desired. For some applications a linearized signal is more suitable, which can be achieved with previously demonstrated methods[30]. Moreover, buffering is often used for FDML applications[31], which means that the SOA is modulated in a way, such that the light which is transmitted through the filter changes its frequency nearly linear. We recorded the beat note signal between the FDML laser and the monochromatic laser, which resulted in a transient beat note signal appearing at the crossing points in wavelength and time (Fig. 2a, b). This resulted in a beat note signal length limited by the bandwidth of the detection (63 GHz). For a total sweep span of 40 nm, we thus were able to observe the phase evolution of 1,7% of the sweep (Fig. 2c). Since the beat signal only constitutes a fraction of the sweep, the wavelength change can be assumed to be linear. The beat note is a frequency-chirp from high frequencies to zero frequency and back (Fig. 2d, e), resulting from the wavelength sweep of the FDML laser. This allows investigation of the temporal evolution of the beat note signal over 126 GHz (−63 GHz to 63 GHz), i.e. double the detection bandwidth. We recorded with a record length of 32 MSamples leading to a total measurement covering 83 consecutive sweeps. This permits the analysis of the temporal evolution of both intra- and inter-sweep signals.

The data were analysed to test for the phase locking stability within the three occurring regimes: The chirped phase leading to the wavelength sweep, the phase of a single mode over consecutive sweeps and the phase evolution of all colours over consecutive sweeps. We thus represent these measurements by three terminologies (cf. Supplementary Note 1): (i) swept phase continuity, (ii) single-mode phase evolution and (iii) all-mode phase evolution. The analysis of (i) the swept phase continuity permits insight into the phase chirp characteristic, i.e. how a single sweep is chirped over all colours (cf. Fig. 2d, e and Supplementary Note 2). (ii) Single-mode phase evolution is used to analyse the phase revisitation error (or jitter) from sweep-to-sweep, i.e. how well a certain colour (or mode) is revisited at the same time over consecutive sweeps (cf. Fig. 3). Importantly, it further allows testing for a comb structure and a carrier-envelope phase slip (CEPS) of the FDML laser. (iii) Finally, the all-mode phase evolution permits investigation of the global phase evolution both between colours and along consecutive sweeps, i.e. how well all colours are phase-locked over intra-sweep and inter-sweep times (cf. Fig. 4). Finally, a numerical analysis is presented to simulate the FDML laser in sweet spot mode and compare it with a non-dispersion compensated FDML laser (cf. Fig. 5).

Swept phase continuity. First, we analysed the swept phase continuity. By zooming into the beat signal, it is visible that the swept phase evolution is continuous and does not exhibit discontinuities (Fig. 2d, e and Supplementary Note 2). A more complete representation by plotting the phase accumulation over the sweep using a Hilbert transform is presented in Supplementary Note 3 and shows the expected behaviour of a decelerated and accelerated phase accumulation due to the swept phase of the FDML laser relative to the monochromatic CW laser.

Single-mode phase evolution. Secondly, we investigated the phase evolution of one mode, i.e. one colour of the sweep, over time (Fig. 3). Therefore, all 83 recorded sweeps (Fig. 3a) were overlaid by starting them at a single time point relative to the start of a sweep. A zoom-in of this overlay is shown in Fig. 3b, which
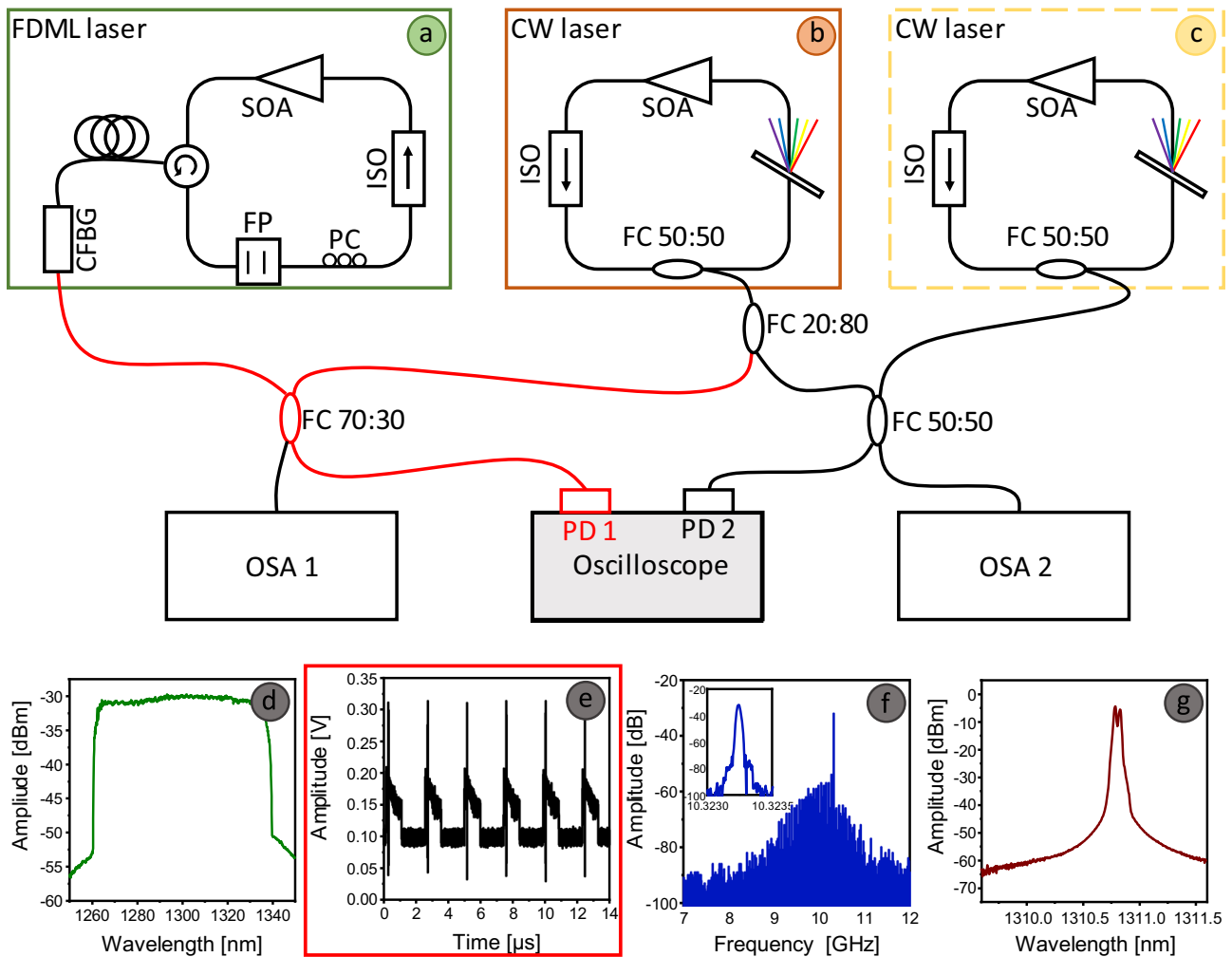
Fig. 1 Setup for beat signal measurements. The core of the investigation is the superposition of the temperature stabilized Fourier domain mode-locked (FDML) laser (**a**) and one continuous wave (CW) laser (**b**) as shown in red. An auxiliary CW laser (**c**) is superimposed with the first one to simultaneously generate a second beat signal to monitor the short-term linewidth of the CW lasers. One optical spectrum analyser (OSA 1) is used to monitor the spectrum of the FDML laser (**d**). The transient beat signals between FDML laser and CW laser (**e**) are measured on a photodiode PD 1 and recorded with a fast real-time oscilloscope (shaded rectangle). The time trace of the second beat signal was measured on the second channel of the oscilloscope with a photodiode PD 2. A live Fourier transform was performed on the signal showing the radio frequency spectrum (**f**) to estimate an upper limit of the convoluted linewidth of both CW lasers. Only measurements for which this second monitoring signal shows a narrow linewidth were used for the analysis of the FDML laser, because only then we can assume that the CW laser had a sufficiently narrow linewidth to see fluctuations on the FDML laser's linewidth. For easy tuning of the CW lasers to generate a certain desired beat frequency, their optical spectra (**g**) were detected with OSA 2. The optical spectrum of both CW lasers corresponds to the shown ~10.3 GHz beat note frequency. SOA = semiconductor optical amplifier, ISO = optical isolator, PC = polarization controller, FP = tunable Fabry-Pérot filter, CFBG = chirped fibre Bragg grating, FC = fibre coupler, PD = photodiode, OSA = optical spectrum analyser.

however only visualizes five consecutive sweeps for better visibility. By analysing the phase at a single time-point along a sweep (i.e. ideally the phase of a single mode), we observed an oscillatory motion of this phase (Fig. 3c). This behaviour would be expected even for a perfectly phase-locked FDML laser, as already the beating with the CW laser will contribute a phase slip since experimentally the absolute frequency of the CW laser was not fixed to an integer multiple of the FDML repetition rate. This sinusoidal oscillation indicates that the FDML output represents a well-defined sweep to sweep phase characteristic, i.e. distinct laser modes separated by the FDML repetition rate in a frequency comb-like structure. However, a few minor discontinuities are visible (Fig. 3c). The FDML repetition rate and therefore the mode frequency spacing between the modes changes over time due to a not perfect temperature stabilization. Since this temperature drift is slow[29], here, the mode frequency spacing does not change within one measurement. To quantitatively analyse

the instantaneous linewidth and thus the coherence of the single-mode (i.e. the phase revisitation error), we performed a fast Fourier transform (FFT) of this single-mode phase evolution oscillation (Fig. 3d) which results in a linewidth of 12 kHz in the presented dataset. The actual instantaneous linewidth of the FDML laser might even be lower as the spectrum corresponds to a convolution of the spectra of the CW and the FDML laser. Therefore, the instantaneous linewidth of 12 kHz as an upper limit indicates an instantaneous coherence length of at least 25 km (see methods). The numerical simulation of an FDML laser in sweet-spot operation yields a linewidth of 6 kHz, i.e. close to the experimental value.

All-mode phase evolution. To analyse the overall phase behaviour of the FDML laser output for all colours over many sweeps, the all-mode phase evolution is shown in Fig. 4. For all time
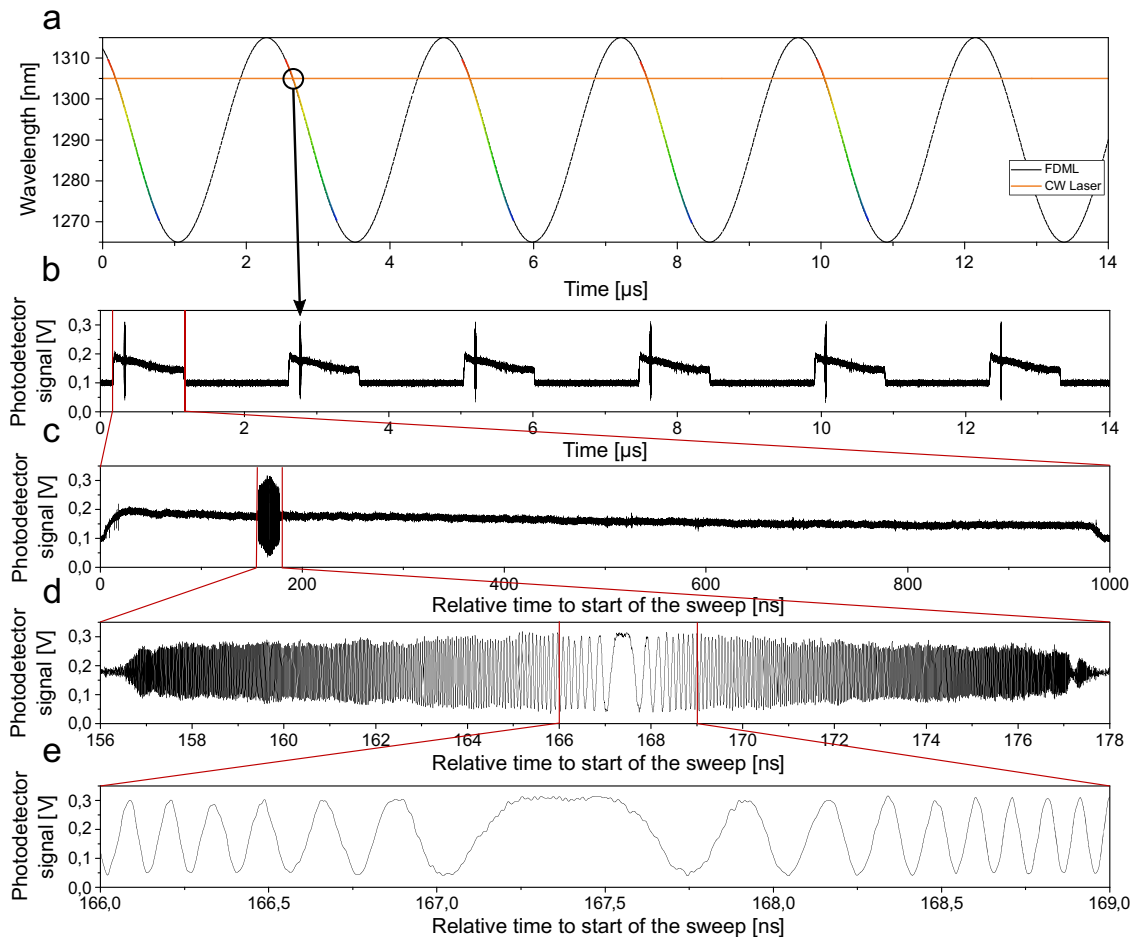
Fig. 2 Swept phase continuity measurements to determine the chirped phase characteristics of Fourier domain mode-locked laser. The Fourier domain mode-locked (FDML) sweep can be idealized by a sinusoidal sweep in wavelength (**a**). The continuous wave (CW) laser is a monochromatic laser, represented here by a constant wavelength over time. Thus, around the intersection points, a beat note signal can be measured by a fast oscilloscope. The experimental data of this beat note signal is shown in (**b**). Due to the repetitive behaviour of the swept source FDML, this beat signal occurs periodically with the roundtrip frequency. **c** Zoom into one FDML sweep where the beat signal occurs over an optical bandwidth of 0.7 nm (±0.35 nm). This is limited by the electronic detection bandwidth of 63 GHz (see methods). **d** Zoom into the beat signal reveals the chirped signal with the zero frequency point at approximately 167.4 ns. **e** Zoom into the middle of the beat signal. The beat signals provide an insight into the swept phase continuity of the FDML laser.

points along the overlaid sweeps (Fig. 4a), a single-mode phase evolution (Fig. 4b) and its FFT (Fig. 4c) were calculated as described in Fig. 3. The peak of the FFT curves for all modes (Fig. 4c) was utilized to generate a graph showing the phase slip for all modes over all times, i.e. the phase evolution for all modes and all times (Fig. 4d). The flatness of the graph is an indication for a stable CEPS and therefore coupled modes. We see that the phase change is nearly the same for each roundtrip, which is direct evidence for stable phase locking. Due to mode hops of the CW laser between measurements different datasets can show different CEPS (Fig. 4e) despite all parameters being the same (see methods).

Numerical simulations. The hypothesis that the FDML laser constitutes a frequency comb or at least presents a comb-like structure can experimentally currently only be investigated indirectly. Thus, we performed a theoretical, numerical simulation to have full access to the coherence properties, the phase evolution and analyse the influence of the chromatic dispersion in the laser cavity. Figure 5a shows the simulated all-mode phase evolution for several dispersion values, ranging from 0 fs to 1900 fs residual dispersion for the optical bandwidth of 40 nm around 1290 nm and

a dispersion-engineered cavity length of ~500 m single-mode fibre (see methods)[29]. The simulation results for 150 fs residual dispersion resembles the experimental results from Fig. 4d, which is in agreement with our previous findings that a sweet spot operation of FDML lasers is obtained with residual dispersion values below 200 fs[29]. However, even with higher than optimal dispersion values, the simulation shows smooth all-mode phase evolution plots which implies a certain phase relation between the swept modes. When analysing the simulated FDML sweeps for a frequency comb structure (Fig. 5b, c), a comb-like structure is visible. The dispersion-optimized, sweet spot FDML shows a high-fidelity comb-structure with 411 kHz comb spacing (corresponding to the sweep repetition rate) and comb linewidth values (full width at half maximum, FWHM) of ~6 kHz (inset in Fig. 5b), which is determined by remaining long-term drifts in the laser field. This value is roughly a factor of two lower than the one presented measured value for residual phase variations of 12 kHz (FWHM) which additionally contains a contribution of the CW laser (cf. Fig. 3d). The broadening of the comb lines in the non-dispersion-compensated case can be attributed to the non-stationary high-frequency fluctuations in the intensity trace[26,29,32], which are absent in the ultra-stable regime. It is important to note that the experimental measurement utilizes a time gate window width of 6.25 ps, which corresponds to ~100 comb lines
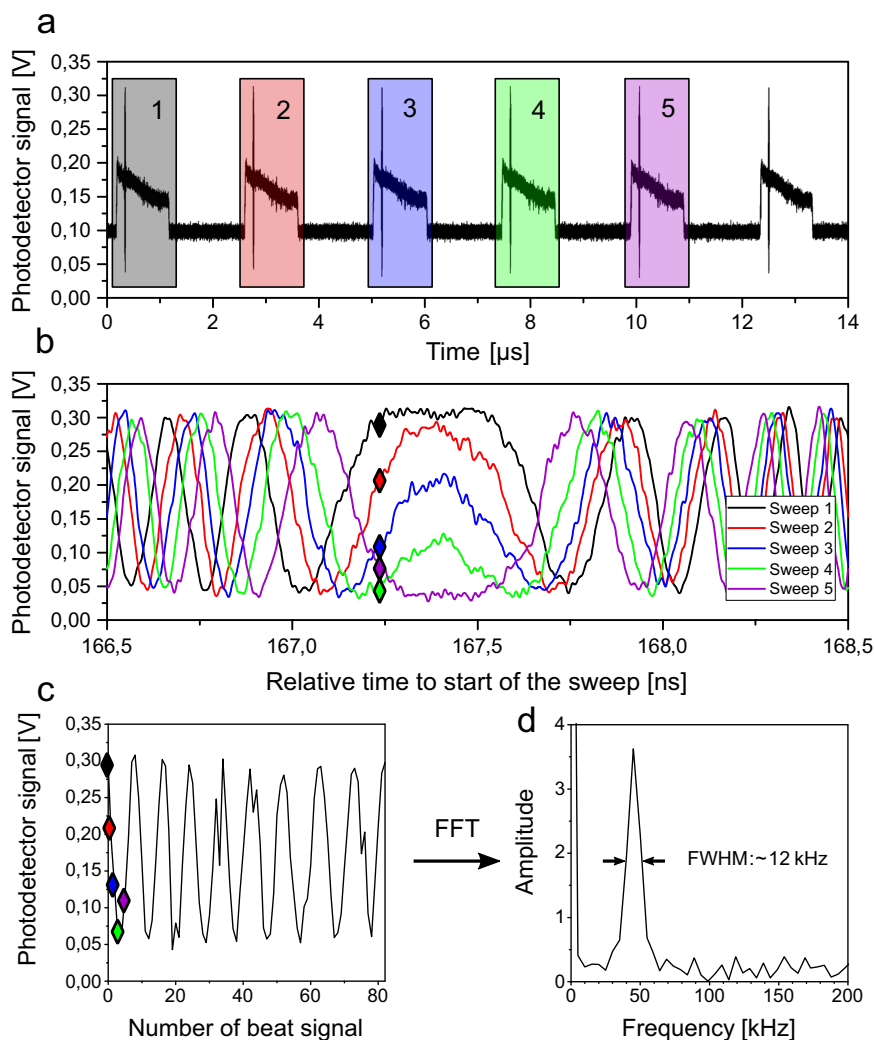
Fig. 3 Analysis of the phase evolution for a single longitudinal mode of the Fourier domain mode-locked (FDML) laser. Consecutive sweeps (**a**) were overlaid (**b**) to gain access to the phase of a single longitudinal mode and its evolution from sweep to sweep. Oscillatory behaviour is observed (**c**) when plotting the phase evolution at a single time point relative to the sweep starts (here at 167,25 ns). **d** A fast Fourier transform (FFT) reveals an oscillation frequency of 44,6 kHz. This oscillatory behaviour can be explained by a phase slip between the continuous wave (CW) laser and the FDML laser since the optical frequency of the CW laser is not necessarily an integer multiple of the FDML sweep repetition rate. However, also a carrier-envelope phase slip (CEPS) of the FDML laser could be present and convoluted in this observed oscillation. The smooth nature of the observed phase oscillation indicates a constant phase slip that accumulates linearly over consecutive sweeps. This leads to the conclusion that the FDML laser output represents a comb-like structure.

simultaneously (see methods). Thus, the measured linewidth is a convolution of ~100 beat note measurements occurring simultaneously and thus the determined value of 12 kHz only represents an upper value for the linewidth of a single comb line. As can be seen in Fig. 5c, even a sub-optimally configured FDML laser cavity with large residual chromatic dispersion exhibits a comb-like structure with even comb spacing.

Based on our simulation results, it can be concluded that the FDML laser operating in the ultra-stable regime has a mode structure and that a coherence over at least 1000 roundtrips exists, resulting in a frequency comb spectrum. The numerical simulation confirms the hypothesis and the experimental findings that the single longitudinal modes are mode-locked with a stable phase relation both along the chirped wavelength sweep (swept phase continuity, Fig. 2) as well as over consecutive sweeps (Figs. 3 and 4). Chirped frequency combs have recently gained tremendous attention in the context of quantum cascade lasers[33–35], operating in the mid-infrared and terahertz regimes. Our results indicate that Fourier domain mode-locking in the

ultra-stable regime might offer a possibility to produce chirped frequency combs in the near-infrared.

Conclusion

In summary, we confirmed both experimentally and theoretically that the FDML laser constitutes a (not stabilized) frequency comb structure. Currently, the experimental approach only permits an indirect measurement via light-beating with a CW laser. This is not optimal, since this measurement is a convolution of the FDML CEPS and the phase slip induced by the two non-phase-locked lasers. Thus, here no direct CEPS measurement was possible. In future setups, the CW laser can be phase-locked to the FDML repetition rate for a direct CEPS measurement to enable locking this CEPS and thus generating a stabilized FDML frequency comb. It might also be speculated about a setup based on amplitude modulation of the FDML output light and amplification of the resulting pulses[20] to measure the offset frequency of an FDML comb. The pulses may be used to generate a
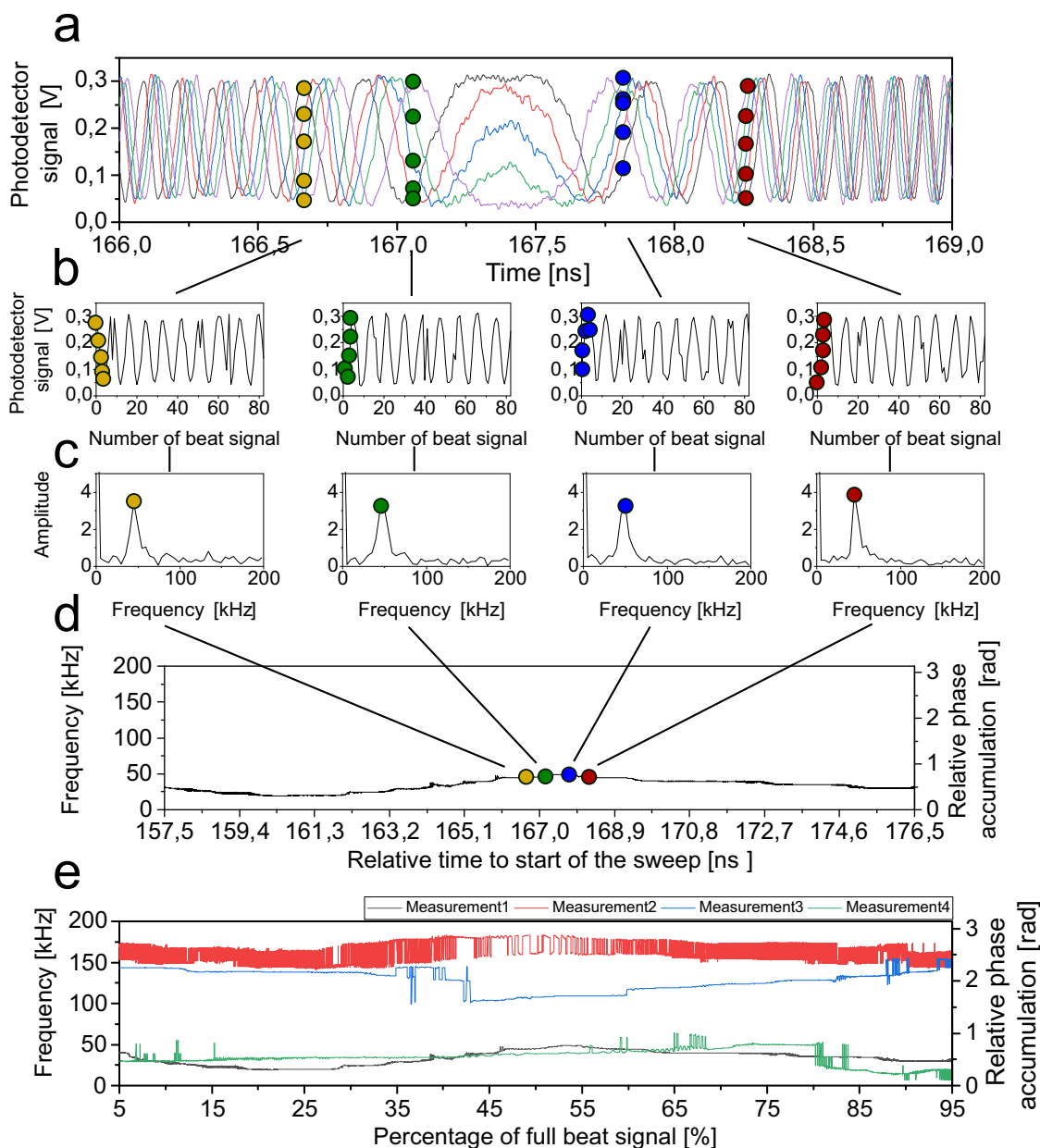
Fig. 4 All-Mode phase evolution experimental data. By analysing 83 consecutive sweeps, it is possible to analyse the phase evolution over all modes and many sweeps. We overlaid successive sweeps (**a**), generated single-mode phase evolutions (**b**) and calculated the fast Fourier transform (FFT)s (**c**) for each timepoint similar to the analysis in Fig. 3. Here, four exemplary modes are indicated by coloured circles. The phase evolution for all modes and all times is presented in (**d**) as a plot of the FFT frequency maximum over the time points. This plot reveals that the individual modes have a distinct and smooth phase relation between each other and over consecutive sweeps. Thus, we deduce that the Fourier domain mode-locked laser (FDML) laser output represents a well-defined wavelength sweep with a continuously chirped phase light field both along a sweep (i.e. from mode-to-mode) and over multiple sweeps (i.e. from sweep-to-sweep). **e** We repeated this measurement several times and found that the phase always has a connected and locally smooth shape apart from a step-like resolution artefact which is sometimes visible and is likely caused by the limited frequency resolution due to the finite record length of the measurement (see Supplementary Note 4 for discussion). We also found that the averaged frequency value drastically changes from measurement to measurement even if all parameters were the same. That is due to continuous wave (CW) laser mode hops in between measurements. Slight changes within the frequency evolution could be traced back to changes in the FDML light field. Larger changes between different measurements could be traced back to small alterations of the CW ring laser wavelength.

supercontinuum in a photonic crystal fibre which is then used in a typical f-2f beat setup to measure the carrier-envelope slip. Such an absolute frequency normal with ~52 million comb lines will enable new applications in high-resolution spectroscopy in form of a time-frequency ruler, where the frequency of an unknown signal can be determined precisely by the exact time-to-wavelength encoding provided by the FDML laser[17].

Furthermore, this FDML frequency comb output can already now be utilized for broad range, arbitrary frequency synthesis especially in the Terahertz range. Further, this manuscript showed that the FDML laser is ideally suited for high-speed spectro-temporal imaging with ultra-low spatial jitter due to the high phase stability of the time-to-wavelength sweep characteristic[19,21]. Lastly, a CEPS-stabilized FDML laser will
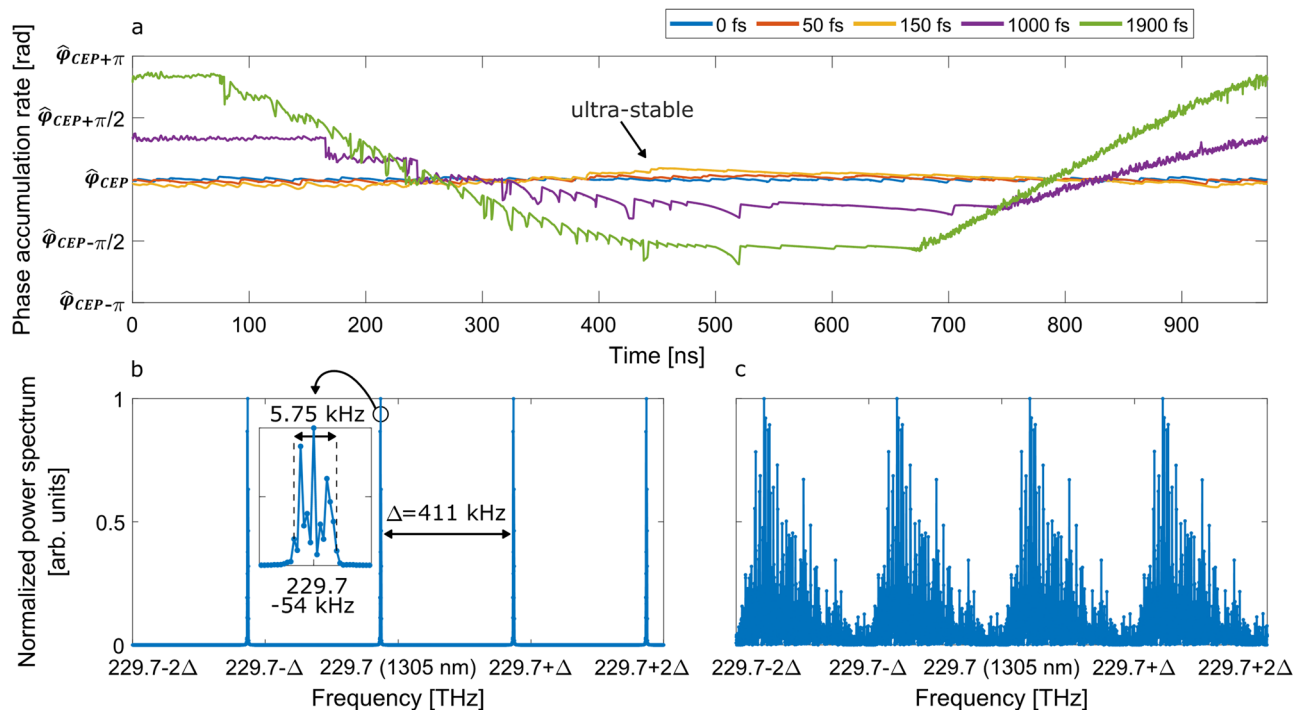
Fig. 5 Numerical simulation of the Fourier domain mode-locked (FDML) output. a The all-mode phase evolution plot presents the relative phase accumulation per roundtrip of the FDML laser and is plotted for various values of residual dispersion in the fibre cavity (see legend). The curves show good agreement with the experimental data in Fig. 4 since the ultra-stable regime and the connected small dispersion exhibit a constant carrier-envelope phase slip (CEPS). Higher dispersion induces a non-constant CEPS. By simulating up to 1000 consecutive sweeps it is possible to investigate the frequency spectrum at optimal spectral resolution and reveal a comb-like structure of the FDML laser output (**b**). In the ultra-stable regime[28,29] (i.e. negligible dispersion effects, here residual dispersion of 150 fs) the FDML laser presents a stable frequency comb with fixed carrier-envelope offset, i.e. without CEPS from sweep-to-sweep. Thus, a frequency comb is present with mode spacing corresponding to the sweep repetition rate (i.e. 411 kHz). Zoom into a comb-line (inset in (**b**)) reveals a linewidth of 5.75 kHz. This is in good agreement with the experimentally determined, resolution-limited linewidth of 12 kHz (Fig. 3d), which however stems from a simultaneous beating of ~100 spectral modes within the sampling gate window width (see methods). **c** For a non-dispersion compensated FDML laser cavity (residual dispersion of 192 ps) the comb lines are broadened as a result of high-frequency fluctuations (Nozaki-Bekki holes) in the intensity trace and the loss of coherence[24,26,29,32]. The good agreement between theory and experiment confirms the observed comb-like structure of the FDML and paves the way towards an FDML frequency comb with a stabilized carrier-envelope offset.

provide an electro-optical link between the electronic sweep repetition rate in the kHz regime to the optical ~230 THz regime and can thus open up new applications in optical metrology and spectroscopy.

Methods

FDML laser. The home-built, temperature-stabilized FDML laser consists of a semiconductor optical amplifier (SOA, BOA 1132 S, Thorlabs), a fibre-based delay line cavity, mostly consisting of HI1060 fibre, and a home-built fibre based tuneable Fabry-Pérot optical bandpass filter (FP). A chirped fibre Bragg grating (CFBG) is used for dispersion compensation. An optical isolator (ISO) ensures unidirectional operation, and a polarization controller (PC) is used to optimize the polarization and hence the lasing and the laser power. The filter is periodically tuned synchronously to the optical roundtrip frequency of 411 kHz. The filter drive frequency is actively controlled by a closed feedback loop over a few 10ths of mHz to compensate remaining drift caused by imperfect cavity temperature stabilization, which has a short time stability of ~0.01 °C (see Fig. 4 in Pfeiffer et al.[29]). With an actively controlled sweep frequency the FDML laser can be kept in sweet spot operation mode[28,29]. In sweet spot operation or ultra-stable regime FDML lasers hardly exhibit any excess intensity noise. In typical FDML lasers it can be achieved when the remaining dispersion of the ~500 m long fibre cavity is less than ~200 fs[29]. In short, this is achieved with a chirped fibre Bragg grating, careful selection of the fibre types and a temperature gradient at the grating. The centre wavelength of the FDML laser is 1300 nm and the maximum achievable sweep bandwidth, limited by the gain width of the SOA, is 140 nm. For a longer beat signal the bandwidth was smaller: 40 nm for the presented data in Fig. 2, Fig. 3 and measurement 1 and 2 in Fig. 4 and 80 nm in measurement 3 and 4 in Fig. 4. The FDML laser output is modulated with a duty cycle of 40%. Usually, the laser is operated with a duty cycle of 12,5%, but it has been extended to obtain a longer beat signal.

CW laser. The two identical tuneable ring laser cavities each consist of a semiconductor optical amplifier (SOA, BOA1132, Thorlabs) and an optical isolator (ISO), connected by polarization-maintaining fibres. A free space beam path with tiltable transmission gratings (GTI25-03A, Thorlabs) serves as a tunable wavelength-selective element. A fibre coupler (FC) serves as output. The lasers are operated in continuous wave mode, the wavelength can be adjusted from ~1240 nm–1380 nm. By superimposing the light of the two CW lasers their stability and linewidth are monitored. The two lasers were always set to a wavelength difference of about 0.05 nm to generate a 10 GHz beat signal. The optical spectra are measured with an OSA and their interference signal is detected with a photodiode (Discovery Semiconductors DSC20H, 35 GHz, PD 2) and the real-time oscilloscope. If both lasers have no mode hops during measurement, the Fourier transform of this beat signal has a narrow tall peak and one laser can be used for the superposition with the FDML laser. The CW laser's short-term linewidth is <10 kHz.

Measurement setup. The superposition of FDML and CW laser is detected with a fast photodiode from Finisar (XPDV2320R, 50 GHz 3 dB roll-off, PD 1). The data is recorded with a 63 GHz real-time oscilloscope (DSOZ634A Infiniium, Keysight). The raw data is freely available online[36]. We note that a measurement with a radio frequency spectrum analyser would only record a time-averaged signal due to the fast sweep rate of up to >10^19 Hz s^−1 of the FDML laser. Additionally, the high speed of the oscilloscope allows to fully characterize the light field of the FDML laser, as this frequency represents the upper limit of the laser output noise. This is due to the unique setup of the FDML principle, where the optical bandpass filter of the intra-cavity Fabry-Pérot-filter acts as a low-pass filter for the maximum frequency of phase and amplitude fluctuations. The filter with an optical bandwidth of ~0.165 nm corresponds to a frequency limiter of only ~29 GHz at 1300 nm. Therefore, any optical phase or amplitude fluctuations from the laser are slower than the electronic bandwidth of the detection. The OSA to measure the optical spectrum of the FDML laser is from Hewlett Packard (86142 A). The spectra of the CW lasers are detected with an OSA from Yokogawa (AQ6370).

The beat signal measurement is a superposition of the ideal harmonic wave of the ring laser

$$E_{CW}(t) = A_{CW} \cdot e^{i \cdot 2\pi \cdot \nu_{CW} t + \varphi_{CW}} \qquad (1)$$

and a chirped signal

$$E_{FDML}(t) = A_{FDML} \cdot e^{i \cdot 2\pi \cdot \nu_{FDML}(t) \cdot t + \varphi_{FDML}} \qquad (2)$$

of the FDML laser. The sweep operation of the FDML laser follows closely the tuning operation of the intra-cavity filter. This is a Fabry-Pérot filter with sinusoidal tuning, so the wavelength is given by $\lambda(t) = \lambda_0 + C \cdot \sin(2\pi\nu_{FDML} \cdot t)$ where λ_0 is the centre wavelength and C the half tuning range. Since we only analyse about 20 ns out of a 2.4 µs filter tuning cycle, we can linearize the instantaneous FDML frequency to $\nu_{FDML}(t) = \nu_0 + \alpha \cdot t$ where α is a constant in Hz s^{-1} indicating the change in optical frequency of the FDML laser per second. ν_0 is the starting frequency of the FDML laser, A_{CW} and A_{FDML} the amplitudes of CW and FDML laser, ν_{CW} the frequency of the CW laser and φ_{CW} and φ_{FDML} are absolute phase offsets of the CW and FDML laser.

Swept phase continuity. The FDML laser is modulated with a duty cycle of 40% (rainbow in Fig. 2a). Within a sweep the wavelength changes from 1310 nm to 1270 nm (backward sweep). The wavelength of the CW laser is 1305 nm. Beat signal traces were measured for 200 µs or 83 successive sweeps. The beat signals were tenfold upsampled through zero padding in the frequency domain for better visibility of the smooth swept phase continuity especially at the edges of the beat signals. It was verified that the upsampling did not change the results of the following data analysis methods.

Single-mode phase evolution. The trace is cut every 2.4 µs, corresponding to the reciprocal of the FDML repetition rate of 411 kHz. Successive sweeps were overlaid, and the amplitude was compared at one time-point (Fig. 3a, b) generating a periodic phase evolution (Fig. 3c). An FFT is applied to this single-mode phase evolution. The revealed spectrum is a convolution of the spectrum of the FDML laser and the spectrum of the CW laser. Since the single-mode phase evolution is made of one data point per beat signal, the sampling rate corresponds to the FDML frequency of 411 kHz. Therefore, the Nyquist frequency is 205.5 kHz and the frequency resolution is 4.95 kHz. The linewidth of the superposition of the two CW lasers was 9 kHz. Since this is also a convolution of the spectra of the two single CW lasers, it is only an upper limit for the linewidth of one of the CW lasers. The presented instantaneous linewidth of 12 kHz is the specific value for the presented dataset at the presented spectral position. We measured somewhat different values in the range of 5 kHz to 25 kHz depending on the spectral position and the dataset.

The shown spectra of the single-mode phase evolution are amplitude spectra, which are used to determine the instantaneous linewidths. Usually, the linewidth is determined from the power density spectrum, i.e. the squared amplitude spectrum. The linewidth in the amplitude spectrum and the corresponding power density spectrum differs by a factor $\sqrt{2}$ if a Gaussian-shaped spectrum is given. The shape of the spectrum is unknown. Moreover, the linewidths are in the range of the frequency resolution and are only estimates. Therefore, it is of secondary importance from which spectrum the linewidth is determined. Due to the unknown spectral shape $L_c = c / \triangle\nu$ with coherence length L_c, speed of light c and linewidth $\triangle\nu$ is used to determine an estimation of the coherence length.

Despite choosing the name single-mode phase evolution for the phase evolution at one point in time over consecutive sweeps we could not measure single modes. The consecutive sweeps of an FDML laser with a sweep span of 40 nm comprise 17.5 million modes. The 0.7 nm and 21 ns long beat signals include 307,000 laser modes. Therefore, the 6.25 ps gate width of the fast oscilloscope contains more than 100 comb lines.

All-mode phase evolution. The data in Fig. 4d, e were generated as follows. The beat signals were overlaid for the evaluation of the single-mode phase evolution, but the amplitude not at one time point but for all data points of a beat signal was compared, generating as many single-mode phase evolution plots as data points are present. The edges of the beat signal (around 5% on each side), where the amplitude starts to decrease, are not evaluated. Each was Fourier transformed. The frequencies with the maximum amplitude in every spectrum were detected by fitting a parabola through the highest data point and its neighbours on both sides. The frequency resolution of around 5 kHz generates numerical artifacts, which are explained in the Supplementary Note 4. The frequencies with the maximum amplitude (besides the zero frequency part) are then plotted over time. Figure 4e shows all-mode phase evolution plots for different datasets and laser parameters. Here the percentage of a full beat signal is used as x-axis since the beat signals are of different lengths. In measurements 1 and 2 the FDML laser had a bandwidth of 40 nm and the CW laser had a wavelength of 1305 nm. Measurement 1 originates from the dataset presented in Figs. 2 and 3., where approximately 3000 data points within the range from 157.5 ns to 176.5 ns were analysed. In measurements 3 and 4 the FDML laser had a bandwidth of 80 nm around 1290 nm and the CW laser had a wavelength of 1290 nm. Therefore, the beat signal is shorter and contains approximately 1300 data points. The sweep range in measurements 3 and 4 is 80 nm, but the total sweeps also last approximately 1 µs. The beat signal is

evaluated over 8 ns. The visible sweep in measurements 1 and 2 is approximately 21 ns long and evaluated over 19 ns due to the shorter sweep range of 40 nm. The graphs in Fig. 4d, e present the phase change with each roundtrip over the beat signal (relative phase accumulation), whereas 205.5 kHz corresponds to π. However, a specific value cannot be determined as the exact frequency of the CW laser is unknown. Note, all-mode phase evolution includes all modes within the beat signal, not all modes within a sweep. The number of the modes is limited by the beat frequency bandwidth.

Simulations. Simulations are based on the model from Schmidt et al.[26] with a centre sweep wavelength of 1290 nm and a sweep bandwidth of 40 nm similar to the data in Fig. 2. 1000 consecutive roundtrips were analysed extracted from a laser setup operated in the ultra-stable or sweet-spot regime as in the case of the experimental data and the results compared to lasers operating beyond the ultra-stable regime. Here the intensity trace is distorted by high-frequency fluctuations[26,29,32]. The amount of dispersion in the fibre delay cavity was varied in order to take into account an imperfect dispersion compensation. The fibre dispersion is a dominant noise source in FDML lasers[29] and serves here as a model for non-synchronized operating conditions. As shown in the publication from Schmidt et al.[26] the laser can still run in the ultra-stable regime up to a threshold of group delay in the fibre cavity due to the dynamics induced by the swept Fabry Pérot filter. Since timing delays caused by the residual dispersion in the fibre cavity accumulate over time, this phenomenon strongly indicates that the optical phase is locked in the ultra-stable regime as shown by the measurement results of Figs. 2–4.

The beat signal $E_{beat}(t)$ of Eqs. (1) and (2) which is proportional to the optical power incident on the photodetector, i.e. $\propto |E_{CW}(t) + E_{FDML}(t)|^2$, can be computed to be

$$E_{beat}(t + nT_R) \propto \cos\left[2\pi\nu_{FDML}(t)t - 2\pi(t + nT_R)\nu_{CW} + \varphi_{FDML}(t + nT_R) - \varphi_{CW}\right]. \qquad (3)$$

We choose $t \in [0, T_R]$ with the roundtrip time T_R and express arbitrary points in time by adding the roundtrip number n times the roundtrip time. From Eq. (3) it follows that if the FDML laser has a periodically varying instantaneous with period T_R, apart from a constant phase accumulation per roundtrip $\varphi_{FDML}(t + nT_R) = n \bullet \varphi_{CEP}$ with the carrier-envelope phase slip φ_{CEP}, the beat signal is $\propto \cos(n\varphi_{beat} + \varphi_{const})$.

Here

$$\varphi_{beat} = \varphi_{CEP} - 2\pi\nu_{CW}T_R \qquad (4)$$

and

$$\varphi_{const} = 2\pi[\nu_{FDML}(t_0) - \nu_{CW}]t_0 - \varphi_{CW} \qquad (5)$$

when tracking the beat signal at an arbitrary point in the sweep t_0 over consecutive roundtrips as depicted in Fig. 3.

This simple model based on idealized signals is able to explain the measured beat signal from Fig. 4a. Note that the measured beat signal also contains a contribution of the CW laser, which prohibits a direct observation of the CEPS of the FDML laser from our measurement. Our simulation confirms the constant phase accumulation of the optical field over the entire sweep, which is an extension to Fig. 4d where a stable beat signal was presented in a 19 ns window of the 1 µs long sweep. The phase accumulation $\hat{\varphi}_{CEP}$ of the FDML laser extracted from our simulation is shown in Fig. 5a for different amounts of residual dispersion in the fibre cavity. The residual dispersion is characterized by the maximum group delay difference between the fastest and slowest wavelength in the fibre cavity. Here we traced the phase of the optical field in the swept-filter reference frame[13] over 100 roundtrips and computed the phase difference between consecutive roundtrips at each point in the entire sweep, where a maximum deviation from a constant rate was identified to be below 0.05 rad for all traces in the ultra-stable regime. The optical phase in the swept-filter reference frame contains all phase fluctuations induced by the laser components apart from constant contributions of the group-phase offset[37], the Fabry Pérot filter mirrors[38] or the CW laser as mentioned above. This means that the absolute phase accumulation rate φ_{beat} as measured in Fig. 4 cannot be extracted from the simulation but is equal apart from a constant offset to $\hat{\varphi}_{CEP}$ in Fig. 5a. The fundamental advantage of the swept-filter reference frame is the possibility to analyse the residual noise in the entire sweep bandwidth. This is impractical for the full field due to the large time-bandwidth product in the order of $\approx 10^7$ which is reduced by three orders of magnitude in the reference frame. For comparison to the ultra-stable case, the average phase accumulation rate for a residual dispersion of 1000 fs and 1900 fs is included in Fig. 5a, when the intensity trace of the laser is distorted by non-stationary high-frequency intensity fluctuations, i.e. when not all of the modes are locked. The evolution follows the parabolic phase accumulation induced by the fibre dispersion, which can be extracted from the model of Schmidt et al[26]., and is not compensated in this regime. Single sweet-spots still exist in the intensity trace due to single wavelengths synchronized with the sweep rate as shown by Pfeiffer et al.[29] and are visible as constant lines in Fig. 5a.

Since an ideal periodic signal possesses a comb spectrum in the Fourier domain, we Fourier transformed 1000 consecutive roundtrips, equivalent to an observation

time of 2.4 ms, of an ultra-stable as well as a non-dispersion-compensated laser. We analysed the spectrum of the full field in a small window around 1305 nm, corresponding to the wavelength of the CW laser in Figs. 2–4, due to the limited simulation bandwidth as discussed above. Therefore, we have further verified our results at various positions in the sweep. The spectra around 1305 nm are presented in Fig. 5b, c. Even in the non-dispersion-compensated case in Fig. 5c, which has been shown to be a stationary lasing regime[13], a quasi-mode structure is observed. The width of these modes can significantly be reduced in the ultra-stable regime in Fig. 5b to near-ideal comb lines (see inset in Fig. 5b), consistent with the stable phase slip in the experiment demonstrated in Fig. 3.

Data availability

The datasets generated and analysed during the current study are available in the Zenodo repository, https://doi.org/10.5281/zenodo.6561441.

Code availability

For our central conclusions no complex custom, specialized or unique code or mathematical algorithms were used.

References

1. Huber, R., Wojtkowski, M. & Fujimoto, J. Fourier Domain Mode Locking (FDML): A new laser operating regime and applications for optical coherence tomography. *Opt. Express* **14**, 3225–3237 (2006).
2. Huber, R., Taira, K., Wojtkowski, M. & Fujimoto, J. G. Fourier Domain Mode Locked Lasers for OCT imaging at up to 290 kHz sweep rates. In *Optical Coherence Tomography and Coherence Techniques II.* (ed. Drexler, W.) Vol. 5861 of Proc. SPIE (Optica Publishing Group, 2005), paper PDA3.
3. Swanson, E. A. & Fujimoto, J. G. The ecosystem that powered the translation of OCT from fundamental research to clinical and commercial impact. *Biomed. Opt. Express* **8**, 1638–1664 (2017).
4. Kolb, J. P. et al. Live video rate volumetric OCT imaging of the retina with multi-MHz A-scan rates. *PLoS ONE* **14**, e0213144 (2019).
5. Klein, T., Wieser, W., Eigenwillig, C. M., Biedermann, B. R. & Huber, R. Megahertz OCT for ultrawide-field retinal imaging with a 1050nm Fourier domain mode-locked laser. *Opt. Express* **19**, 3044–3062 (2011).
6. Blatter, C. et al. Ultrahigh-speed non-invasive widefield angiography. *J. Biomed. Opt.* **17**, 070505 (2012).
7. Mohler, K. J. et al. Combined 60 wide-field choroidal thickness maps and high-definition en face vasculature visualization using swept-source megahertz OCT at 1050 nm. *Investig. Ophthalmol. Vis. Sci.* **56**, 6284–6293 (2015).
8. Wang, T. et al. Heartbeat OCT: in vivo intravascular megahertz-optical coherence tomography. *Biomed. Opt. Express* **6**, 5021–5032 (2015).
9. Cecchetti, L. et al. In-vitro and in-vivo imaging of coronary artery stents with Heartbeat OCT. *Int. J. Cardiovas. Imaging* **36**, 1021–1029 (2020).
10. Wang, T. et al. Intravascular optical coherence tomography imaging at 3200 frames per second. *Opt. Lett.* **38**, 1715–1717 (2013).
11. Blatter, C. et al. In situ structural and microangiographic assessment of human skin lesions with high-speed OCT. *Biomed. Opt. Express* **3**, 2636–2646 (2012).
12. Strenge, P. et al. Registration of histological brain images onto optical coherence tomography images based on shape information. *Phys. Med. Biol.* **67**, 135007 (2022).
13. Jirauschek, C., Biedermann, B. & Huber, R. A theoretical description of Fourier domain mode locked lasers. *Opt. Express* **17**, 24013–24019 (2009).
14. Biedermann, B. R., Wieser, W., Eigenwillig, C. M., Klein, T. & Huber, R. Dispersion, coherence and noise of Fourier domain mode locked lasers. *Opt. Express* **17**, 9947–9961 (2009).
15. Kranendonk, L. A. et al. High speed engine gas thermometry by Fourier-domain mode-locked laser absorption spectroscopy. *Opt. Express* **15**, 15115–15128 (2007).
16. Karpf, S., Eibl, M., Wieser, W., Klein, T. & Huber, R. Shot-Noise Limited Time-Encoded Raman Spectroscopy. *J. Spectroscop.* **2017**, 9253475 (2017).
17. Karpf, S., Eibl, M., Wieser, W., Klein, T. & Huber, R. A Time-Encoded Technique for fibre-based hyperspectral broadband stimulated Raman microscopy. *Nat. Commun.* **6**, 1–6 (2015).
18. Chen, D., Shu, C. & He, S. Multiple fiber Bragg grating interrogation based on a spectrum-limited Fourier domain mode-locking fiber laser. *Opt. Lett.* **33**, 1395–1397 (2008).
19. Karpf, S. et al. Spectro-temporal encoded multiphoton microscopy and fluorescence lifetime imaging at kilohertz frame-rates. *Nat. Commun.* **11**, 1–9 (2020).
20. Karpf, S. & Jalali, B. Fourier-domain mode-locked laser combined with a master-oscillator power amplifier architecture. *Opt. Lett.* **44**, 1952–1955 (2019).
21. Jiang, Y., Karpf, S. & Jalali, B. Time-stretch LiDAR as a spectrally scanned time-of-flight ranging camera. *Nat. Photonics* **14**, 14–18 (2020).
22. Jirauschek, C. & Huber, R. Efficient simulation of the swept-waveform polarization dynamics in fiber spools and Fourier domain mode-locked (FDML) lasers. *JOSA B* **34**, 1135–1146 (2017).
23. Slepneva, S. et al. Dynamics of Fourier domain mode-locked lasers. *Opt. Express* **21**, 19240–19251 (2013).
24. Slepneva, S. et al. Convective Nozaki-Bekki holes in a long cavity OCT laser. *Opt. Express* **27**, 16395–16404 (2019).
25. Li, F. et al. Eckhaus instability in laser cavities with harmonically swept filters. *J. Lightwave Technol.* **39**, 6531–6538 (2021).
26. Schmidt, M., Pfeiffer, T., Grill, C., Huber, R. & Jirauschek, C. Self-stabilization mechanism in ultra-stable Fourier domain mode-locked (FDML) lasers. *OSA Contin.* **3**, 1589–1607 (2020).
27. Holzwarth, R. et al. Optical frequency synthesizer for precision spectroscopy. *Phys. Rev. Lett.* **85**, 2264 (2000).
28. Kraetschmer, T. & Sanders, S. T. Ultrastable Fourier Domain Mode Locking Observed in a Laser Sweeping 1363.8–1367.3 nm. In *Conference on Lasers and Electro-Optics/International Quantum Electronics Conference, OSA Technical Digest (CD).* (Optica Publishing Group, 2009), paper CFB4.
29. Pfeiffer, T., Petermann, M., Draxinger, W., Jirauschek, C. & Huber, R. Ultra low noise Fourier domain mode locked laser for high quality megahertz optical coherence tomography. *Biomed. Opt. Express* **9**, 4130–4148 (2018).
30. Eigenwillig, C. M., Biedermann, B. R., Palte, G. & Huber, R. K-space linear Fourier domain mode locked laser and applications for optical coherence tomography. *Opt. Express* **16**, 8916–8937 (2008).
31. Huber, R., Adler, D. C. & Fujimoto, J. G. Buffered Fourier domain mode locking: unidirectional swept laser sources for optical coherence tomography imaging at 370,000 lines/s. *Opt. Lett.* **31**, 2975–2977 (2006).
32. Schmidt, M. et al. Intensity pattern types in broadband Fourier domain mode-locked (FDML) lasers operating beyond the ultra-stable regime. *Appl. Phys. B* **127**, 60 (2021).
33. Singleton, M., Jouy, P., Beck, M. & Faist, J. Evidence of linear chirp in mid-infrared quantum cascade lasers. *Optica* **5**, 948–953 (2018).
34. Hillbrand, J., Andrews, A. M., Detz, H., Strasser, G. & Schwarz, B. Coherent injection locking of quantum cascade laser frequency combs. *Nat. Photonics* **13**, 101–104 (2019).
35. Opačak, N. & Schwarz, B. Theory of Frequency-Modulated Combs in Lasers with Spatial Hole Burning, Dispersion, and Kerr Nonlinearity. *Phys. Rev. Lett.* **123**, 243902 (2019).
36. Huber, R. et al. Original raw data to paper "Towards Fourier Domain Mode Locked frequency combs". https://doi.org/10.5281/zenodo.6561441 (2022).
37. Helbing, F. W., Steinmeyer, G. & Keller, U. Carrier-envelope offset phase-locking with attosecond timing jitter. *IEEE J. Sel. Top. Quantum Electron.* **9**, 1030–1040 (2003).
38. Jirauschek, C. & Huber, R. Wavelength shifting of intra-cavity photons: Adiabatic wavelength tuning in rapidly wavelength-swept lasers. *Biomed. Opt. Express* **6**, 2448–2465 (2015).

Author contributions

R.H. conceived the concept of beat signal measurements. T.P. build the FDML laser with the assistance of W.D., who provided the FFP driver amplifier. D.K. and T.B. build the CW lasers. D.K., T.P., T.B., and C.G. conducted the beat signal measurements. D.K., T.P., and C.G. created new software for data analysis. C.G. and D.K. performed data analysis. T.B., C.G., and M.S. performed visualizations. M.S. conducted the simulations. C.G., S.K. and M.S. wrote the manuscript. J.P.K. substantively revised the manuscript. C.J. conceived and supervised the simulations. R.H. supervised the research.

Competing interests

T.P.: Optores GmbH (E, P, R), WD: Optores GmbH (I), R.H.: Optores GmbH (I, P, R), Abott (P, R) with E: employed, P: Patent, R: royalties, I: shares. Relevant patents: US

7414779 B2—issued. Mode locking methods and apparatus: This patent describes the concept of Fourier Domain Mode Locking. Inventor: R.H.; owner: Massachusetts Institute of Technology. DE 10 2017 209 739 B3—issued. Verfahren zur Erhaltung der Synchronität eines Fourier Domain Mode Locked (FDML) Lasers: This patent describes a regulation loop for FDML sweet spot operation: Inventors: T.P., R.H.; owner: University of Lübeck. The other authors declare no competing interests.

Additional information

Supplementary information The online version contains supplementary material available at https://doi.org/10.1038/s42005-022-00960-w.

Correspondence and requests for materials should be addressed to Robert Huber.

Peer review information *Communications Physics* thanks Chang Seok Kim and the other, anonymous, reviewer(s) for their contribution to the peer review of this work. Peer reviewer reports are available.

Reprints and permission information is available at http://www.nature.com/reprints